



K-Co-Mo-S_x Chalcogel – High Capacity Removal of Pb²⁺ and Ag⁺ and their Underlying Mechanisms

Journal:	<i>Journal of Materials Chemistry A</i>
Manuscript ID	TA-ART-07-2024-005158.R1
Article Type:	Paper
Date Submitted by the Author:	30-Sep-2024
Complete List of Authors:	Nie, Jing; Jackson State University Roy, Subrata; Jackson State University, Department of Chemistry, Physics and Atmospheric Sciences Dhami, Sital; Jackson State University, Department of Chemistry, Physics and Atmospheric Sciences Islam, Taohedul; Jackson State University, Department of Chemistry, Physics, and Atmospheric Sciences Amin, Ruhul; Oak Ridge National Laboratory, Electrification and Energy Infrastructure; ORNL Zhu, Xianchun; Jackson State University, Department of Civil Engineering Taylor-Pashow, Kathryn; Savannah River National Laboratory Han, Fengxiang; Jackson State University, Islam, Saiful; Jackson State University, Chemistry, Physics, and Atmospheric Sciences

K-Co-Mo-S_x Chalcogel: High-Capacity Removal of Pb²⁺ and Ag⁺ and the Underlying Mechanisms

Jing Nie^{1,‡}, Subrata Chandra Roy^{1,‡}, Sital Dhami¹, Taohedul Islam,¹ Ruhul Amin², Xianchun Zhu³, Kathryn Taylor-Pashow,⁴ Fengxiang X. Han¹, Saiful M. Islam^{*,1}

¹Department of Chemistry, Physics and Atmospheric Sciences, Jackson State University, Jackson, Mississippi, USA

²Electrification and Energy Infrastructures Division, Oak Ridge National Laboratory, Hardin Valley Campus, Knoxville, TN, 37830, USA

³Department of Civil Engineering, Jackson State University, Jackson, Mississippi, USA

⁴Savannah River National Laboratory, Aiken, SC-29808, USA

[‡]Joint first author

ABSTRACT

Chalcogenide-based aerogels, known as chalcogels, represent a novel class of nanoparticle-based porous amorphous materials characterized by high surface polarizability and Lewis base properties, exhibiting promising applications in clean energy and separation science. This work presents K-Co-Mo-S_x (KCMS) chalcogel as a highly efficient sorbent for heavy metal ions and details its sorption mechanisms. Its incoherent structure comprises Mo₂^V(S₂)₆ and Mo₃^{IV}S(S₆)₂ anion-like clusters with four- and six-coordinated Co—S polyhedra, forming a Co-Mo-S covalent network that hosts K⁺ ions through electrostatic attraction. Interactions of KCMS with heavy metal ions, particularly Pb²⁺ and Ag⁺, revealed that KCMS is exceptionally effective in removing these ions from ppm concentrations down to trace levels (≤5 ppb). KCMS rapidly removes Ag⁺ (≈81.7%) and Pb²⁺ (≈99.5%) within five minutes, achieving >99.9% removal within an hour, with a distribution constant, K_d ≥ 10⁸ mL/g. KCMS exhibits an impressive removal capacity of 1378

mg/g for Ag^+ and 1146 mg/g for Pb^{2+} , establishing it as one of the most effective materials known to date for heavy metal removal. This material is also effective for the removal of Ag^+ and Pb^{2+} along with Hg^{2+} , Ni^{2+} , Cu^{2+} , and Cd^{2+} from various waters even in the presence of highly concentrated and chemically diverse cations, anions, and organic species. Analysis of the post-interacted KCMS by synchrotron X-ray pair distribution function (PDF), X-ray photoelectron spectroscopy (XPS) and energy dispersive X-ray spectroscopy (EDS) revealed the sorption of Pb^{2+} , Ag^+ , and Hg^{2+} mainly occurs by the exchange of K^+ and Co^{2+} . Despite being amorphous, this material exhibits unprecedented ion-exchange mechanisms both for the ionically and covalently bound K^+ and Co^{2+} , respectively. This discovery advances our knowledge of amorphous gels and guides material synthesis principles for the highly selective and efficient removal of heavy metal ions from water.

Keywords: chalcogels, heavy metal remediation, wastewater, ion-exchange

Synopsis: Disordered aggregated porous nanoparticles of KCMS are highly efficient and have exceptionally high sorption capacity in removing silver and lead cations following the exchange of potassium and cobalt cations bonded electrostatically and covalently in KCMS, respectively.

INTRODUCTION

The industrial revolution has substantially accelerated the demand for indiscriminate exploitation of global resources, thereby worsening environmental crises worldwide.¹ Among the array of industrial pollutants, heavy metal-containing wastewater remains a focal concern because of their improper handling and disposal leading to their release into water and subsequent contamination of the ecosystem. Heavy metals are generally harmful to biological systems, including humans, with certain ones such as lead, mercury, silver, and cadmium posing significant risks, including carcinogenicity, neurocognitive disorders, and DNA damage to human health even at trace levels.^{2–7} Hence, it is of utmost importance to decontaminate wastewater containing heavy metals before discharging it into the environment.

In recent years, numerous methods, such as electrocoagulation (EC),⁸ adsorption,^{9,10} membrane separation,^{10,11} magnetic field implementations,¹² electrokinetic extraction,¹³ ion-exchange¹⁴ and others were introduced to remove heavy metals from water. Among the various chemical approaches, ion exchange is potentially viable for the decontamination of water because of its superiority in selectivity and efficiency in separating heavy metal ions from wastewater.^{15–18} Different materials, such as zeolite, activated carbon, biochar, polymer, biomaterials, resin, and layered double hydroxides have been used for heavy metals removal.^{19–25} While these materials demonstrate some degree of effectiveness in separating numerous heavy metals, they often exhibit poor selectivity, efficiency, sorption kinetics, and capacity. Also, their shortcomings become evident when addressing the challenge of removing heavy metals at trace levels from water.

Sulfur-based materials exhibit superior affinity towards heavy metal ions²⁶ and possess the capability to selectively bind Lewis acidic soft heavy metal ions, following Pearson's hard-soft Lewis acid-base principles (HSAB).²⁷ Consequently, this class of materials has emerged as efficient sorbents for soft heavy metal cations, such as Hg^{2+} , Pb^{2+} , Ag^+ , Cu^{2+} , and Cd^{2+} enabling their selective separation even at trace levels. In recent years, chemically and structurally diverse metal sulfides have been investigated in removing soft or relatively soft heavy metal cations. These materials include layered metal sulfides: $\text{K}_{2x}\text{Mn}_x\text{Sn}_{3-x}\text{S}_6$ (KMS-1),^{15,28} $\text{H}_{2x}\text{Mn}_x\text{Sn}_{3-x}\text{S}_6$ (LHMS-1),²⁹ $\text{K}_{2x}\text{Mg}_x\text{Sn}_{3-x}\text{S}_6$ (KMS-2),¹⁶ $\text{K}_{2x}\text{Sn}_{4-x}\text{S}_{8-x}$ (KTS-3),¹⁷ open framework structures, such as $\text{K}_6\text{Sn}[\text{Zn}_4\text{Sn}_4\text{S}_{17}]$,³⁰ $[(\text{Me})_2\text{NH}_2]_2[\text{GeSb}_2\text{S}_6]$,³¹ metal sulfide intercalated layered double hydroxides, and chalcogels.^{32,33}

Among them, chalcogel, an emerging class porous nanoparticle-based amorphous materials, stands out remarkably because of its unique structural skeleton consisting of polysulfides, which finds great affinity toward chemically soft Lewis acidic cations.³⁴⁻³⁶ Structurally, chalcogels typically comprise monomeric units of (metal-)chalcogenides, interconnected through either chalcogen-chalcogen or metal-chalcogenide covalent bonds and thus integrate high-density (poly)sulfide into its nanoparticles. Hence, the incorporation of alkali metals into the covalent networks of metal-sulfide can introduce electrostatic bonding features. This leads to the formation of hybrid chalcogels consisting of covalent and ionic bonds. This can represent a distinct class of porous nanomaterials with ion-exchange properties akin to crystalline metal sulfides, including $\text{K}_{2x}\text{M}_x\text{Sn}_{3-x}\text{S}_6$ ($\text{M} = \text{Mn}$, KMS-1; $\text{M} = \text{Mg}$, KMS-2),^{15,16} $\text{K}_{2x}\text{Sn}_{4-x}\text{S}_{8-x}$ ($x = 0.65-1$),¹⁷ and

$\text{K}_6\text{Sn}_5\text{Zn}_4\text{S}_{17}$ ³⁰ which shows ion-exchange properties toward chemically soft Lewis acidic heavy metal ions.³⁷ This characteristic holds promise for potential applications in wastewater treatment and the extraction of critical metals from water sources.

Here, we present the significant potential of K-Co-Mo-S_x chalcogel for effectively separating heavy metal cations from aqueous solutions. This material exhibits over 99.9% removal of Ag⁺ and Pb²⁺ from initial concentrations of about 10⁴ ppb, with the distribution constants of $K_d \geq 10^8$ mL/g in just an hour. Besides, KCMS exhibits an enormously high sorption capacity of $q_m^{\text{Ag}} \sim 1378$, $q_m^{\text{Pb}} \sim 1146$, and also for mercury, $q_m^{\text{Hg}} \sim 461$ mg/g. Moreover, KCMS can remove Ag⁺, Hg²⁺, and Pb²⁺ from ppm to trace level (≤ 5 ppb) from naturally contaminated wastewater systems. Despite being amorphous, this material exhibits double ion-exchange properties for ionically and covalently bound K⁺ and Co²⁺, respectively. Overall, the integration of rapid, high-capacity removal of heavy metals, alongside room temperature-scalable synthesis and an unprecedented adsorption mechanism, demonstrates the transformative potential of chalcogels in wastewater treatment.

RESULTS AND DISCUSSIONS

Synthesis and characterization: K-Co-Mo-S_x chalcogel was synthesized via a redox-driven metathesis route in solution at room temperature, following a previously reported procedure (detailed in the SI).³⁸ After the synthesis of the wet-gel, the as-prepared gel in the solution was washed to remove the unreacted spectator ions (Figure 1A). The gel was then dried at room temperature to produce xerogel. Scanning electron microscopy (SEM) images of the xerogel show

homogeneity of the gel particle (Figure 1B). As discussed previously, detailed analysis of the chemical composition by SEM/EDS analysis of the K-Co-Mo-S chalcogel, synthesized from various batches was collected in micrometer length scales, indicating an average atomic abundance of K, Co, Mo, and S as 8.0 ± 2.3 , 7.4 ± 1.7 , 9.4 ± 1.6 , and $74.2 \pm 4.6\%$, respectively and are closely related to results obtained from submicron-level particles determined by TEM/EDS.³⁸ The absence of any sharp diffraction peak in the XRD pattern of the KCMS gels suggests the lack of periodic arrangement in its amorphous structure (Figure 1C). Synchrotron X-ray pair distribution functions analysis shows peaks at 2.03, 2.42, and 2.73 Å which are related to S-S, Mo-S, and Mo-Mo bonding correlations, respectively (Figure 1D). This finding is akin to the previously reported results.³⁸ Previously, we elucidated the local coordination environment of KCMS gels by XPS, HRTEM, TEM-EDS, XANES, and EXAFS analysis.³⁸ Modeling of the Co and Mo K-edges data revealed that six- and four-coordinated Co—S polyhedra linked with Mo—S anionic clusters resembling molecular $\text{Mo}_2^{\text{V}}(\text{S}_2)_6$ and $\text{Mo}_3^{\text{IV}}\text{S}(\text{S}_6)_2$ anions.³⁸ We found that KCMS nanoparticles consist of covalent networks of the Co-Mo-S in which K^+ ions are electrostatically bound to form K-Co-Mo- S_x chalcogel. Hence, the presence of electrostatically bound alkali metals in the covalent network of the Co-Mo-S of the KCMS gels can be ion-exchanged with chemically soft heavy metal cations following the Lewis HSAB principles.²⁷

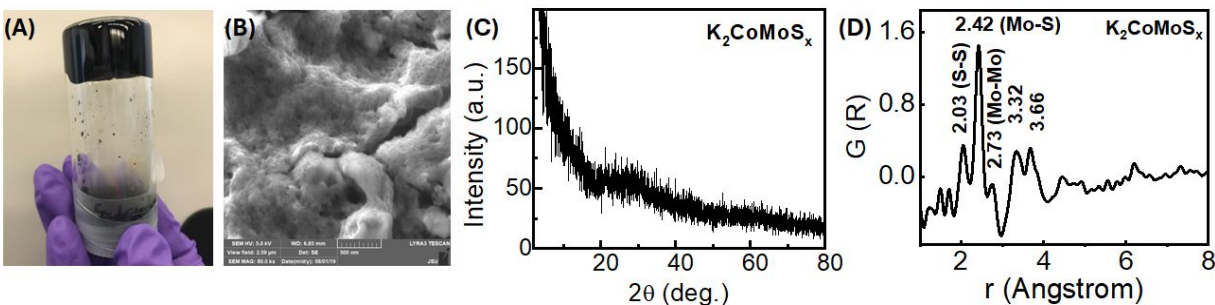


Figure 1. Photograph of the KCMS wet gels (upside down) showing the firmness of the monolith wet gels (A), SEM image of the KCMS xerogel (B), XRD pattern of KCMS xerogel showing amorphous nature of the material (C), PDF analysis of KCMS xerogel demonstrates a short range atomic order with the local coordination of polyhedra (D).

Extraction of Heavy Metal Ions from Aqueous Solutions: We investigated the interactions of the xerogels of KCMS, obtained by drying at ambient conditions, with various transition metal cations that include Cu^{2+} , Hg^{2+} , Ag^{+} , Pb^{2+} , Cd^{2+} , Ni^{2+} , and Zn^{2+} (Table 1). Our studies reveal that KCMS is remarkably efficient for the capture of Ag^{+} , Hg^{2+} , and Pb^{2+} from aqueous solutions. KCMS achieves nearly 100% removal of Ag^{+} and Pb^{2+} in an interaction time of just about an hour with the distribution constant, K_d as high as $\sim 10^8$ mL/g from 10 ppm spiked solutions of metal cations. It also shows effective removal efficiencies for Cu^{2+} and Hg^{2+} , offering removal of ~ 91 and 98%, respectively, with a $K_d > 10^4$ mL/g (Table 1). Such high K_d values suggest a great affinity of the Ag^{+} , Hg^{2+} , and Pb^{2+} for the KCMS chalcogel. It is important to note that any materials with a K_d value in the 10^4 – 10^5 mL/g range are regarded as exceptionally high-quality sorbents.^{17,39} It is important to note that the aerogel form of KCMS which exhibits a surface area of up to 90 m²/g, as reported previously,³⁸ could potentially be more effective due to its high density of pores across the aggregated nanoparticles. However, due to the challenges associated with scalable and cost-

effective synthesis, this study focuses solely on the xerogel form of KCMS.

Table 1: Removal of various heavy metal cations from aqueous solutions by KCMS.

M^{n+}	C_i (ppm)	C_f (ppb)	M^{n+} removal (%)	K_d (mL/g)
Cu^{2+}	10×10^3	872.0	91.30	1.05×10^4
Hg^{2+}	10×10^3	236.8	97.63	4.12×10^4
Ag^+	10×10^3	3.25	99.97	3.08×10^6
Pb^{2+}	10×10^3	0.10	~ 100.0	$\sim 10^8$
Cd^{2+}	10×10^3	9.91×10^3	0.86	8.65
Ni^{2+}	10×10^3	9.12×10^3	8.8	96.49
Zn^{2+}	10×10^3	10×10^3	0.0	0.0

contact time: 1 h, $V = 10.0$ mL; m (mass of KCMS) = 0.01g; V/m ratio = $10/0.01 = 1000$ mL/g.

The competitive sorption analysis of heavy metal cations by KCMS xerogels revealed that only in one hour of interaction, the final concentration of silver ion was reduced from 10,000 to below one ppb, demonstrating an excellent potential of the gels for fast and efficient removal of Ag^+ from aqueous solutions (Table S1). Other heavy metal cations, e.g. Hg^{2+} , and Pb^{2+} , show reasonably good sorption efficiency, whereas other ions show poor to negligible interactions to separate them from water. Based on this result, we found the selectivity order as $Ag^+ > Hg^{2+} > Pb^{2+} \gg Cu^{2+} \gg Ni^{2+} \gg Cd^{2+}$. This finding suggests that KCMS is effective for the selective separation of different heavy metal cations as listed above. This kind of selectivity may be understood by the chemical hardness of these cations. This is because of different binding propensities to chemically soft Lewis basic sulfides of the KCMS with heavy metal ions, as demonstrated by Pearson's Lewis hard and soft acid-base principle.²⁷ This observation is in good agreement with the previously reported

investigation.⁴⁰

Time-dependent experiments for the sorption of Ag^+ , Pb^{2+} , and Hg^{2+} were conducted for KCMS xerogel to determine the removal rate of these metal cations and to understand the mechanism of sorption (Figure 2). The sorption kinetic for Pb^{2+} is ultra-fast. The removal rate of Pb^{2+} cations from the 10^4 ppb spiked solution is 99.51% in 5 minutes and reaches $\sim 100\%$ within 30 min with a K_d value of $\sim 10^8$ mL/g and the final concentration of those heavy metal cations reached < 1 ppb (ng/g). Importantly, such a low concentration for Pb^{2+} is well below the limit for drinking water defined by both the US EPA (15 ppb) and WHO (10 ppb).^{41,42} Furthermore, the removal of Ag^+ and Hg^{2+} reaches about 81.7% and 86.1%, respectively, within 5 minutes and increases to $\sim 97.6\%$ ($K_d \sim 3.8 \times 10^6$ mL/g) and 97.6% ($K_d \sim 4 \times 10^4$ mL/g) within an hour (Table S2). This kind of exceedingly high uptake rate adverts KCMS's potential for the rapid decontamination of Ag^+ , Pb^{2+} , and Hg^{2+} from wastewater. In general, sorption rates and mechanisms can be analyzed by pseudo-first and pseudo-second-order rate equations as described in equations 1 and 2, respectively.⁴³

$$\text{Pseudo-first-order: } \ln(q_e - q_t) = \ln q_e - k_1 t \quad (\text{eq. 1})$$

$$\text{Pseudo-second-order: } \frac{t}{q_t} = \frac{1}{k_2 q_e^2} + \frac{t}{q_e} \quad (\text{eq. 2})$$

Where q_e (mg/g) is the amount of adsorbed element per unit mass of adsorbent at equilibrium and q_t (mg/g) is the adsorbed amount at time t , while k_1 (min^{-1}) and k_2 ($\text{g/mg} \cdot \text{min}^{-1}$) are equilibrium rate constants of pseudo-first-order and pseudo-second-order adsorption interactions, respectively.⁴⁴ Fitting of the experimental data led to a decent linear relationship for the ' t/q_t ' versus ' t ' plot (Figure 2D), demonstrating the sorption of Ag^+ , Pb^{2+} , and Hg^{2+} follow the pseudo-

second-order rate equations where the rate constant, k_2 , for Pb^{2+} is $\sim 3.73 \text{ g/mg}\cdot\text{min}^{-1}$, which is about one and two orders of magnitude higher than that for Ag^+ ($k_2^{\text{Ag}} \sim 0.14 \text{ g/mg}\cdot\text{min}^{-1}$) and Hg^{2+} ($k_2^{\text{Hg}} \sim 0.071 \text{ g/mg}\cdot\text{min}^{-1}$), respectively. (Table S3). Such a higher rate constant is indicative of faster sorption of these ions and agrees with the experimental data (Table S2). The correlation coefficients (R^2) were nearly equal to unity suggesting that KCMS follows pseudo-second-order reaction kinetics for the interactions with Ag^+ , Pb^{2+} , and Hg^{2+} .

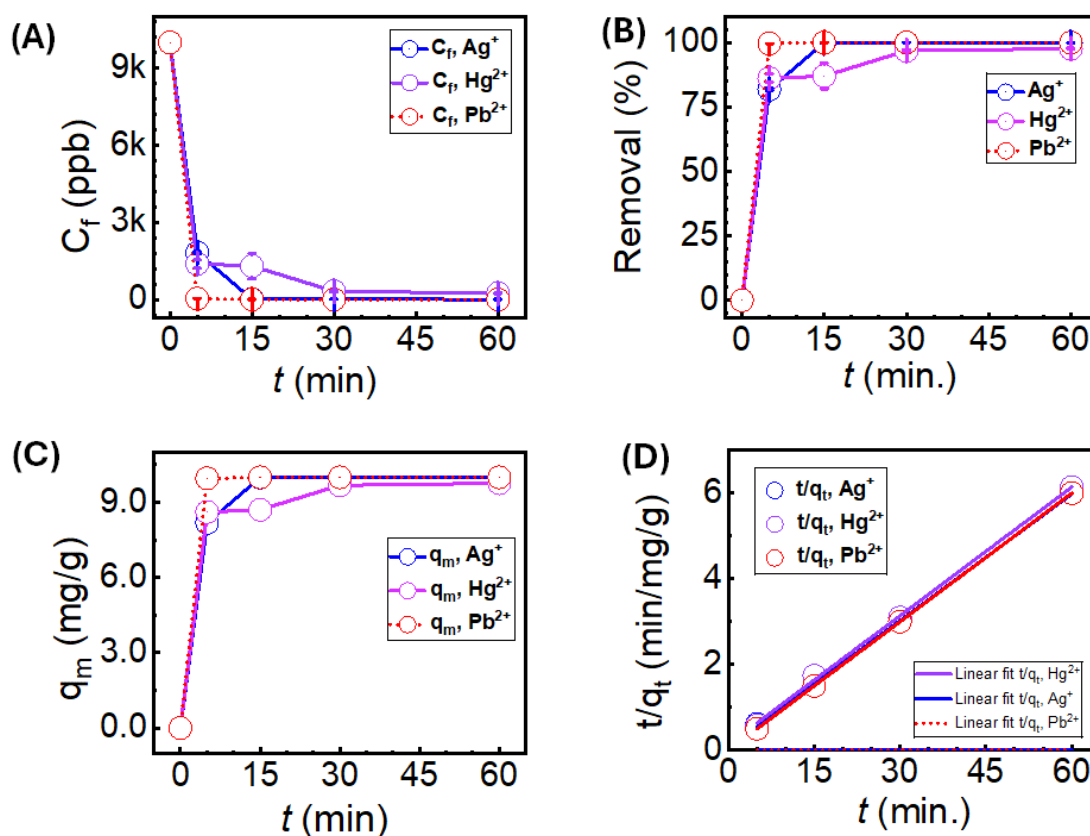
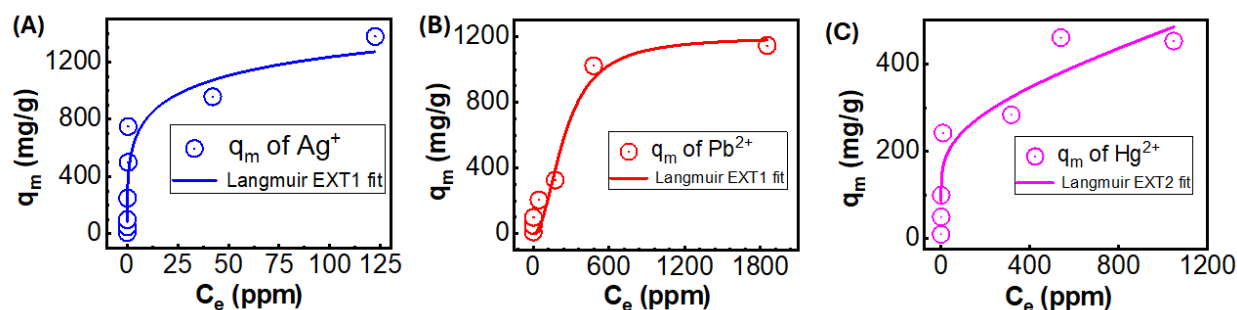


Figure 2. Sorption kinetic for M^{n+} (Ag^+ , Pb^{2+} , and Hg^{2+}) using 10.0 mg of KCMS xerogel in 10 mL of solution: (A) change of $[M^{n+}]$ to the time of interactions, (B) removal % of M^{n+} as a function of time, (C) sorption capacity as a function of contact time, and (D) pseudo-second-order kinetic plots.

To determine the sorption capacity of the KCMS xerogel for Hg^{2+} , Ag^+ , and Pb^{2+} in aqueous solutions, we conducted a concentration investigation and fitted the experimental data with the Langmuir adsorption isotherms model (Figure 3, Table S4). This investigation reveals that KCMS has a remarkably high sorption capacity for Hg^{2+} , Ag^+ , and Pb^{2+} . Our investigations show that KCMS can capture over 87% of Ag^+ from a concentration as high as 1500 ppm with a K_d value of 1.4×10^4 mL/g (Table S4). At this concentration, the maximum sorption capacity was determined to be ~ 1377 mg/g (Figure 3A) where the sorption data were nicely fitted with Langmuir absorption isotherm. This value of q_m^{Ag} is exceptionally high, and stands out as one of the most efficient sorbents among the top materials, such as LDH- Mo_3S_{13} (1073 mg/g),⁴⁵ amorphous MoO_x (2605 mg/g),⁴⁶ LDH- Sn_2S_6 (978 mg/g),³⁹ LDH Ni/Fe/Ti- MoS_4 -LDH (856 mg/g),⁴⁷ Mn- MoS_4 (564 mg/g),⁴⁸ LDH- MoS_4 (550 mg/g),⁴⁹ MoS_4 -ppy (480 mg/g at pH ~ 5),⁵⁰ and Mo_3S_{13} -Ppy (408 mg/g) (Table 2).⁵¹ In addition, our experiment shows that KCMS can remove over 99.5 % of Pb^{2+} with starting concentrations over 100 ppm. The maximum removal capacity of 1146 mg/g was obtained for a spiked solution of 3000 ppm (Figure 3B). Such a tremendously high sorption capacity for Pb^{2+} ranks this material top among the other high-performing Pb^{2+} sorbents, as we can see in Table 2.^{48,49,52–57} We have also investigated the adsorption capacity of Hg^{2+} for solutions of 10 to 1500 ppm. The KCMS affords the removal capacity, $q_m^{\text{Hg}} \sim 460$ mg/g (Figure 3C) which is comparable to other high-performing sorbents as seen in (Table 2). Importantly, KCMS can remove $\geq 99.6\%$ Hg^{2+} from a solution containing as high as 100 ppm of Hg^{2+} (Table S4). Over these concentration ranges (10-100 ppm), the K_d^{Hg} values remain in the range of 10^5 - 10^6 mL/g. Such an exceedingly high K_d demonstrates that KCMS offers paramount potential in the removal of Hg^{2+} from aqueous

211 solutions.



212
213 Figure 3. The sorption capacity of heavy metal cations, Ag^+ (A), Pb^{2+} (B), and Hg^{2+} (C) by KCMS
214 chalcogel was determined by the interaction of 10 mg KCMS with various concentrations of each
215 cation.

216
217 Table 2: Comparison of adsorption capacities for heavy metals with high-performing sorbents
218

Cations	Adsorbents	q_m (mg/g)	References
Ag^+	KCMS	1377	This work
	Amorphous MoO_x	2605	46
	LDH- Mo_3S_{13}	1074	45
	LDH- Sn_2S_6	978	39
	Ni/Fe/Ti- MoS_4 -LDH	856	47
	Mn-LDH- MoS_4	564	48
	MoS_4 -Ppy	480 (pH~5) 725 (pH ~1)	50
	Mo_3S_{13} -ppy	408	51
	MoS_4 -LDH	450	49
	KMS-2	408	58
	Fe- MoS_4	565	52
Pb^{2+}	KCMS	1146	This work
	Lignosulfonate-modified graphene hydrogel	1210	59
	LDH- Sn_2S_6	579	39
	MoS_4 -LDH	290	49
	Mn- MoS_4	357	48
	Fe- MoS_4	345	52
	EDTA-LDH	180	54

	CTS/PAM gel	138	55
	Mg ₂ Al-LS-LDH	123	56
	Cellulose-based chalcogel	240	57
	biomass-based hydrogel	422.7	53
Hg ²⁺	KCMS	460	This work
	LDH-Sn ₂ S ₆	666	39
	MoS ₄ -LDH	500	49
	Mn- MoS ₄	594	48
	Fe-MoS ₄	582	52
	KMS-2	297	58
	MoS ₄ -ppy	210	50
	KMS-1	377	29
	Thio-functionalized magnetic graphene oxide	289	60

Application Potentials: To evaluate the practical use of KCMS xerogel chalcogel for wastewater treatment, we analyzed its removal efficiency for heavy metals using Mississippi River Water (MRW) and Tap Water (TW). Water from both sources was individually spiked with 10 ppm of each metal as listed, Ag⁺, Hg²⁺, Pb²⁺, Ni²⁺, Cu²⁺, and Cd²⁺, resulting in a total concentration of 70 ppm for seven metal ions. Despite the presence of chemically diverse types of species, including high concentrations of cations, anions, and diverse organic species, in those water samples, KCMS can remove Ag⁺, Hg²⁺, Pb²⁺, Ni²⁺, Cu²⁺, and Cd²⁺ (Table 3). Specifically, the removal performance of Ag⁺ and Pb²⁺ from MRW is over 99% and leads to the final concentration of less than 1 ppb. We obtained the selectivity order for tap and Mississippi River water to be Ag⁺ ≈ Pb²⁺ > Hg²⁺ > Cu²⁺ >> Cd²⁺ > Ni²⁺. This finding suggests that KCMS possesses extraordinary potential for the selective separation of Ag⁺ and Pb²⁺ from contaminated waters and thus could be useful for the selective extraction of Ag⁺ and Pb²⁺ from wastewater.

Table 3. Sorption results of KCMS in potable Tap water and Mississippi river water containing seven metal ions of 10 ppm for each (70 ppm total), C_i = initial (pre-sorption) concentration, C_f = final (post-adsorption) concentration.

Mixed-ions	C_i (ppm)	C_f (ppm)	Removal (%)	K_d (mL/g)	q_m (mg/g)	C_f (ppm)	Removal (%)	K_d (mL/g)	q_m (mg/g)
Tap water						MRW			
Cu^{2+}	10.0	3.6184	63.81	1782.4	6.381	3.1254	68.74	2.22×10^3	6.874
Hg^{2+}	10.0	0.2132	97.86	4.60×10^4	9.786	0.1749	98.25	5.68×10^4	9.825
Ag^+	10.0	0.0336	99.66	2.96×10^5	9.966	0.0524	99.48	2.08×10^5	9.948
Pb^{2+}	10.0	0.0686	99.31	1.51×10^5	9.931	0.0279	99.72	3.4×10^7	9.972
Cd^{2+}	10.0	8.0149	19.85	258.65	1.985	8.1857	18.14	2.30×10^2	1.814
Ni^{2+}	10.0	9.5000	4.64	48.63	0.463	9.3766	6.23	6.63×10^1	0.623
Zn^{2+}	10.0	10	0.0	0.0	0.0	10.0	0.0	0.0	0.0

contact time: 24 h, $V = 10.0$ mL; m (mass of KCMS) = 0.01g; V/m ratio = $10/0.01 = 1000$ mL/g

Mechanistic Insights into the Interactions of KCMS with Ag^+ , Hg^{2+} , and Pb^{2+} : To evaluate the sorption mechanisms of $M^{n+} \equiv Ag^+, Pb^{2+}$, and Hg^{2+} ions by KCMS gels, we analyzed the post-reacted sorbent by XRD, PDF, EDS, and XPS. The XRD of the KCMS after interactions with 100 ppm of Ag^+ , Pb^{2+} , and Hg^{2+} cations showed the material remains amorphous (Figure S1). The XRD of the post-interacted materials primarily revealed their amorphousness similar to the pristine KCMS. However, the Ag^+ interacted samples showed weak peak-like humps at $2\theta \sim 15.5$ and 23.0° , which could not be identified. We further analyze the post-treated material by Raman, and TEM for deeper understanding. The strong Raman shift of the pristine KCMS at 487 cm^{-1} (and the shoulder at $\sim 445\text{ cm}^{-1}$) and weak shift at 263 cm^{-1} are attributed to the polysulfide species and K-

247 S bond, respectively³⁸ being missing in the 100 ppm Hg²⁺, Ag⁺, and Pb²⁺ treated material (Figure
248 S2) indicating the ion-exchange and Ag—S—M, Pb—S—M, and Hg—S—M (M=Mo, Co) like
249 interactions. Besides, the TEM images of the Hg²⁺ and Ag⁺ (Figure S3) interacted samples show
250 the aggregation of the particles as expected to the pristine materials. In contrast, the Pb²⁺ interacted
251 sorbent showed a platelike pattern, however, XRD does not reveal the crystalline of the sorbent.
252 Analogous to the pristine KCMS, the PDF of the post-interacted KCMS shows local atomic
253 ordering up to about 6 Å (Figure 4). PDF of KCMS after interactions with 100 ppm of Ag⁺ and
254 Pb²⁺ show a decrease in intensity of the peak at 3.7 Å which is relevant to K⁺···S correlations. Such
255 a reduction in intensity of the 3.7 Å peak can be attributed to a lower concentration of the K⁺ ions
256 in the networks of the KCMS gels suggesting the exchange of K⁺ with Ag⁺ and Pb²⁺. Besides, PDF
257 also shows a decrease in the intensity of S_n²⁻ correlated peaks at ~2.0 Å after interactions with Ag⁺
258 and Pb²⁺ ions. This is due to the breakdown of the S—S bonds of the polysulfide species of the
259 surface exposed chalcogels particles through the formation of Ag—S—M and Pb—S—M bonds,
260 where M is Co or Mo of the KCMS. This finding suggests that besides the ion exchange of K⁺ by
261 Ag⁺ and Pb²⁺, covalent interactions of Ag⁺ and Pb²⁺ with the (—S—S—)_n species of the gel
262 nanoparticles, as —S—Ag/Pb— attribute the sorption of these cations. Besides, although the PDF
263 demonstrates the stability of the KCMS gel's first coordination sphere, the structural changes after
264 sorbent interactions cannot be fully verified due to its amorphous nature. It is also important to
265 note that the sorption of Ag⁺, Pb²⁺, and Hg²⁺ is irreversible, which can be attributed to the stronger
266 M-S (M = Ag⁺, Pb²⁺, Hg²⁺) covalent interactions.

267

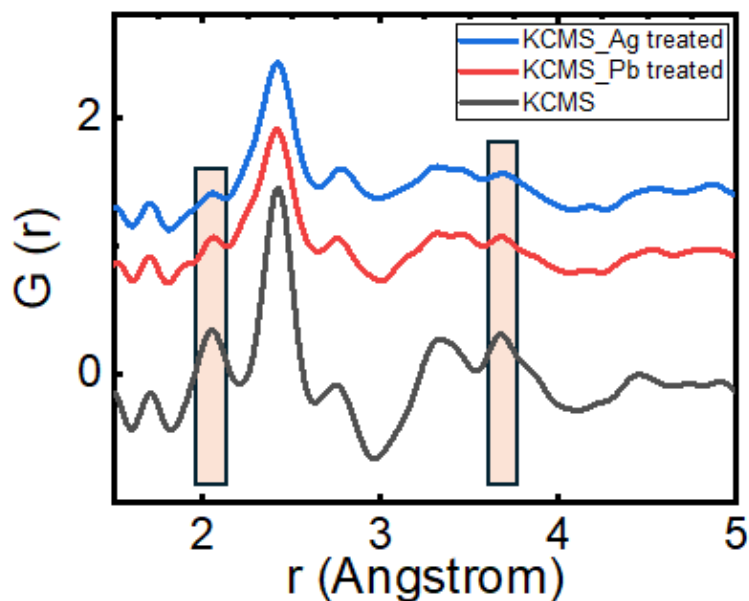


Figure 4: A comparison of the pristine and Ag^+ and Pb^{2+} exposed KCMS showing retention of the local ordering of KCMS gel, light orange shaded lines indicate the change in the intensities between the pristine and Ag^+ and Pb^{2+} exposed samples.

EDS data of KCMS after an interaction of 100 ppm of Ag^+ , Pb^{2+} , or Hg^{2+} ions show the presence of each cation along with a negligible atomic abundance of K^+ ions (Table S5, S6, S7). These findings are likely to suggest that K^+ ions of the KCMS are exchangeable with Ag^+ , Hg^{2+} , and Pb^{2+} ions. It is important to note that the ion-exchange phenomenon was reported for other amorphous chalcogels containing electrostatically bound cations. For example, NH_4^+ of the $(\text{NH}_4)_{0.02}\text{MoS}_x$ ⁶¹ was exchanged by K^+ ions, and Cs^+ and Sr^{2+} cations exchanged K^+ ions of K-Sn-Mo-S gels.²⁶ Apart from this, after the interactions of KCMS with higher concentrations (≥ 1000 ppm) of Ag^+ , Hg^{2+} , and Pb^{2+} the relative atomic abundance of Co decreased by nearly zero percent with the increasing concentration of Ag^+ , Hg^{2+} , and Pb^{2+} (Figure 5, Table S5, S6, S7). For example, after

treating KCMS with 100 and 2000 ppm of Pb^{2+} , the residual atomic abundance of Co ion gradually decreases from $\sim 10\%$ in the pristine KCMS to $\sim 4.4\%$ and 0.2% of Co^{2+} , respectively. A very similar phenomenon was observed for Ag^+ and Hg^{2+} (Figure 5, Table S5, S6, S7). Overall, our experiments showed a decrease in Co^{2+} ion concentration with the increase of the Hg^{2+} , Ag^+ , and Pb^{2+} which may suggest that in addition to K^+ ions, the Co^{2+} ions of the KCMS are also ions exchangeable.

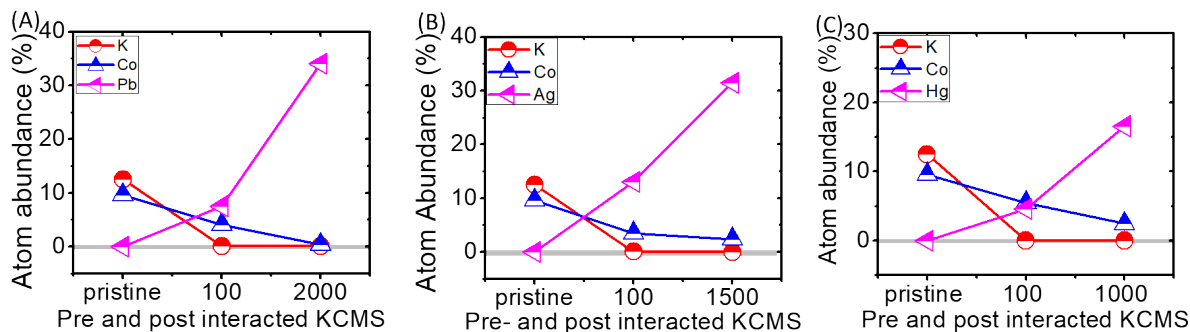


Figure 5. The trend in the change of atomic abundance of K^+ and Co^{2+} ions in KCMS gel with increased concentrations of Ag^+ , Pb^{2+} , and Hg^{2+} .

We also investigated the post-interacted solids after treating them with 100 and ≥ 1000 ppm of Ag^+ , Hg^{2+} , and Pb^{2+} by X-ray Photoelectron Spectroscopy (Figure 6). The XPS of the pristine KCMS shows the presence of a peak centered at 292.1 eV (Figure 6G), which corresponds to K 2p orbital energy.⁶² In contrast, the XPS of the 100 ppm Ag^+ , Pb^{2+} , and Hg^{2+} treated KCMS reveals the absence of a K 2p band but the presence of the bands at 374.0 and 368.0 eV; 104.3 and 100.4 eV; and 143.1 and 138.2 eV (Figure 6 D-F) that correspond to binding energy for Ag^+ ($3d_{3/2}$; $3d_{5/2}$),⁶³ Hg^{2+} ($4f_{5/2}$; $4f_{7/2}$)^{63,64} and Pb^{2+} ($4f_{5/2}$; $4f_{7/2}$)⁶³. The finding suggests the exchange of the K^+ ions of the KCMS by Ag^+ , Pb^{2+} , and Hg^{2+} which also corroborates the EDS findings. Moreover, XPS

spectra of the 100 ppm Ag^+ sorbed solid KCMS show peaks at ~ 779.4 and 782.0 eV (Figure 6A), corresponding to the main and satellite peaks of Co^{2+} 2p orbitals, respectively. In contrast, these peaks at ~ 779.4 and 782.0 eV were absent at the 1500 ppm Ag^+ sorbed KCMS (Figure 6A). Likewise, the Co 2p orbitals peak gradually diminished with an increase in the spiking concentration of Hg^{2+} and Pb^{2+} cations (Figure 6B and C). The above findings imply that polysulfide functional groups have a preferable binding propensity towards softer Ag^+ , Hg^{2+} , and Pb^{2+} cations rather than Co^{2+} cations. Furthermore, the intensities of $3d_{3/2}$ and $3d_{5/2}$ orbitals of Ag^+ , $4f_{5/2}$ and $4f_{7/2}$, orbitals of Hg, and $4f_{5/2}$ and $4f_{7/2}$ orbitals of Pb^{2+} (Figure 6D-F) significantly increase with increasing the spiking concentration of Ag^+ , Hg^{2+} , and Pb^{2+} ion.⁶⁵ This is because of the incorporation of higher concentrations of Ag^+ , Hg^{2+} , and Pb^{2+} in the post-interacted KCMS solids. Hence, EDS and XPS suggest that higher incorporation of Ag^+ , Hg^{2+} , and Pb^{2+} is achieved by the exchange of K^+ and Co^{2+} ions of the KCMS. This kind of double ion exchange for KCMS is chemically driven by the strong affinity of the soft and polarizable Lewis basic sulfide ions toward the soft Lewis acidic Ag^+ , Hg^{2+} , and Pb^{2+} following the Pearson Hard-Soft Lewis Acid-Base paradigm (HSAB).²⁷ Hence a concentration-dependent study shows that KCMS undergoes a preferable ion-exchange at first by the exchange of the electrostatically bound K^+ ions, and then covalently bound Co^{2+} ions. To the best of our knowledge, KCMS is the first example of the amorphous chalcogel that integrates ion-exchange phenomena in both the ionically and covalently bound cations of the chalcogel matrices.

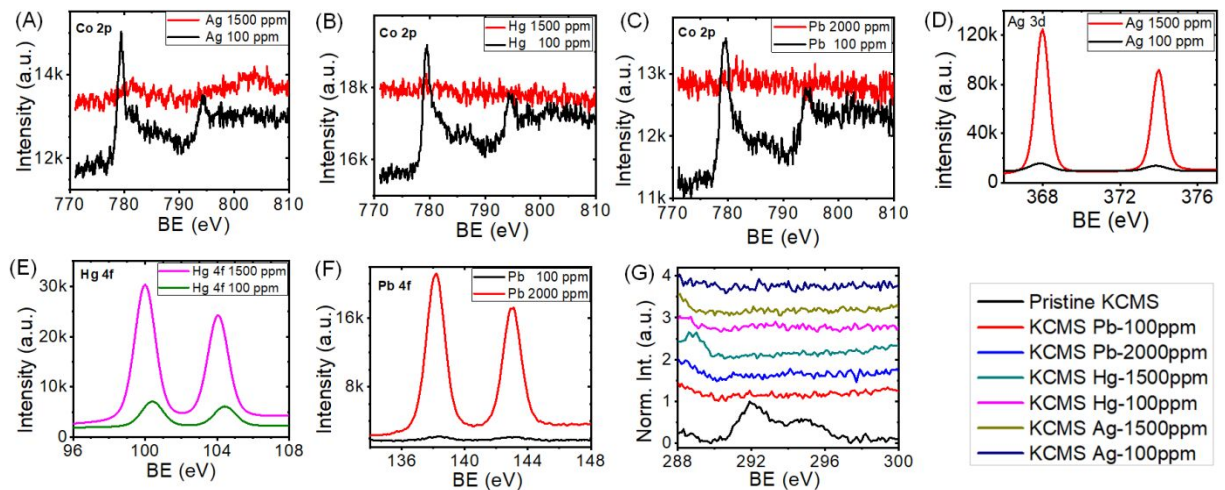


Figure 6: XPS spectra of cobalt 2p (A-C); silver 3d (D); mercury 4f (E); and lead 4f (F); potassium 2p (G) orbitals after interaction of KCMS gels with different concentrations of Ag⁺, Hg²⁺, and Pb²⁺.

It is important to note that the dissolution of cobalt ions from sorbent material can make it unlikely for drinking or household water treatment but could be useful for industrial wastewater treatment of highly toxic Pb²⁺, Hg²⁺, and Ag⁺ for recycling purposes, non-household applications or discharging them into natural water bodies. Apart from this decontamination of Co²⁺ from the KCMS-treated wastewater can be done by the coprecipitation method as the second treatment method. However, this work introduces KCMS as multi-ion exchangeable materials that can exchange both covalently and ionically cations following the Hard-Soft Lewis Acid-Base principles. This finding can potentially open opportunities for designing and synthesizing highly efficient and high-capacity chalcogel-based sorbent using eco-friendly transition metals for cobalt.

CONCLUSIONS

The KCMS chalcogel was synthesized in solution at room temperature. The highly disordered

incoherent structural features of KCMS chalcogels were evidenced by X-ray powder diffraction and Pair Distribution Function (PDF). The KCMS xerogel is highly efficient in removing chemically toxic heavy metal ions, particularly Ag^+ , Hg^{2+} , and Pb^{2+} , achieving over 99.9% removal with a distribution coefficient as high as $\geq 10^8$ mL/g in just half an hour in deionized water solutions. Moreover, Ag^+ , Pb^{2+} , and Hg^{2+} exhibit exceptionally high sorption capacities of 1377, 1146, and 460 mg/g, respectively. Furthermore, we found that this material is exceptionally efficient in removing Ag^+ , Pb^{2+} , and Hg^{2+} from highly contaminated water. For instance, it removes over 99% Ag^+ and Pb^{2+} with a K_d of 10^5 mL/g from the Mississippi River which contains over 10,000 ppb of each cation. The selectivity order observed was $\text{Pb}^{2+} > \text{Ag}^+ > \text{Hg}^{2+} > \text{Cu}^{2+} \gg \text{Cd}^{2+} > \text{Ni}^{2+}$. The remarkable efficiency of KCMS in separating Pb^{2+} and Ag^+ is likely due to the unprecedented and selective ion exchanges of electrostatically bound K^+ and covalently bound Co^{2+} cations and surface sorption. The chemically soft polarizable Lewis basic (poly)sulfide functional groups KCMS offer binding propensities through covalent binding toward Lewis acidic metal cations and the degree of their binding propensity is governed by Pearson's Hard-Soft Lewis Acid-Base (HSAB) paradigm.²⁷ Despite its irreversible sorption properties, KCMS stands out due to its exceptional sorption capacity, fast sorption kinetics, high removal efficiency to trace levels, scalability, solution processability at room temperature, and unique sorption mechanisms, making it an ideal sorbent for chemically soft Lewis acidic heavy metal cations in aqueous solutions. Overall, this study reveals the immense potential of chalcogels for the removal of toxic heavy metal ions and introduces a new paradigm in the design principles of multi-ion-exchangeable chalcogels.

ACKNOWLEDGEMENTS

This work was supported by the US Department of Energy Minority Serving Institution Partnership Program (MSIPP) managed by the Savannah River National Laboratory under BSRA contract (RFP No. 0000542525 and 0000458357). SD is thankful to the NSF Division of Chemistry (NSF-2100797). TI is thankful to the US Department of Energy's Building EPSCoR-State/National Laboratory Partnerships DE-FOA-0002624. This research used resources from the Advanced Photon Source, a U.S. Department of Energy (DOE) Office of Science User Facility operated for the DOE Office of Science by Argonne National Laboratory under Contract No. DE-AC02-06CH11357. The mail-in program at Beamline 11-ID-B contributed to the data.

Data availability

Data for this article, including material Characterization, heavy metal removal performance sorption kinetics, and capacity are available at S. M. Islam, email: Muhammad.s.islam@jsums.edu

Author Contributions

This manuscript was written through the contributions of all authors. All authors have approved the final version of the manuscript.

Conflict of Interest

The authors declare no conflict of interest

Supporting Information

The supporting information file is available: Synthesis and characterization of pristine and post-

sorption KCMS gel by XRD, Raman, EDS, and TEM analysis. Details on uptake study as well as sorption kinetics and capacity of heavy metal analysis by ICP-MS.

Corresponding Author

Saiful M. Islam*

Department of Chemistry, Physics, and Atmospheric Sciences

Jackson State University, Jackson, Mississippi-39217, USA

*E-mail: Muhammad.s.islam@jsums.edu

REFERENCES:

- (1) Türkmen, D.; Bakhshpour, M.; Akgönüllü, S.; Aşır, S.; Denizli, A. Heavy Metal Ions Removal From Wastewater Using Cryogels: A Review. *Front. Sustain.* **2022**, *3*, 765592. <https://doi.org/10.3389/frsus.2022.765592>.
- (2) Naranjo, V. I.; Hendricks, M.; Jones, K. S. Lead Toxicity in Children: An Unremitting Public Health Problem. *Pediatric Neurology* **2020**, *113*, 51–55. <https://doi.org/10.1016/j.pediatrneurol.2020.08.005>.
- (3) Nriagu, J. O.; Blankson, M. L.; Ocran, K. Childhood Lead Poisoning in Africa: A Growing Public Health Problem. *Science of The Total Environment* **1996**, *181* (2), 93–100. [https://doi.org/10.1016/0048-9697\(95\)04954-1](https://doi.org/10.1016/0048-9697(95)04954-1).
- (4) Goldman, L. R.; Koduru, S. Chemicals in the Environment and Developmental Toxicity to Children: A Public Health and Policy Perspective. *Environ Health Perspect* **2000**, *108* (suppl 3), 443–448. <https://doi.org/10.1289/ehp.00108s3443>.
- (5) Needham, L. L.; Barr, D. B.; Caudill, S. P.; Pirkle, J. L.; Turner, W. E.; Osterloh, J.; Jones, R. L.; Sampson, E. J. Concentrations of Environmental Chemicals Associated with Neurodevelopmental Effects in U.S. Population. *NeuroToxicology* **2005**, *26* (4), 531–545. <https://doi.org/10.1016/j.neuro.2004.09.005>.
- (6) Tamasi, G.; Cini, R. Heavy Metals in Drinking Waters from Mount Amiata (Tuscany, Italy). Possible Risks from Arsenic for Public Health in the Province of Siena. *Science of The Total Environment* **2004**, *327* (1–3), 41–51. <https://doi.org/10.1016/j.scitotenv.2003.10.011>.
- (7) Kawata, K.; Osawa, M.; Okabe, S. In Vitro Toxicity of Silver Nanoparticles at Noncytotoxic Doses to HepG2 Human Hepatoma Cells. *Environ. Sci. Technol.* **2009**, *43* (15), 6046–6051. <https://doi.org/10.1021/es900754q>.
- (8) Al-Qodah, Z.; Tawalbeh, M.; Al-Shannag, M.; Al-Anber, Z.; Bani-Melhem, K. Combined Electrocoagulation Processes as a Novel Approach for Enhanced Pollutants Removal: A State-of-the-Art Review. *Science of The Total Environment* **2020**, *744*, 140806. <https://doi.org/10.1016/j.scitotenv.2020.140806>.
- (9) Yang, X.; Wan, Y.; Zheng, Y.; He, F.; Yu, Z.; Huang, J.; Wang, H.; Ok, Y. S.; Jiang, Y.;

- Gao, B. Surface Functional Groups of Carbon-Based Adsorbents and Their Roles in the Removal of Heavy Metals from Aqueous Solutions: A Critical Review. *Chemical Engineering Journal* **2019**, *366*, 608–621. <https://doi.org/10.1016/j.cej.2019.02.119>.
- (10) Qasem, N. A. A.; Mohammed, R. H.; Lawal, D. U. Removal of Heavy Metal Ions from Wastewater: A Comprehensive and Critical Review. *npj Clean Water* **2021**, *4* (1), 36. <https://doi.org/10.1038/s41545-021-00127-0>.
- (11) Van Der Bruggen, B.; Vandecasteele, C.; Van Gestel, T.; Doyen, W.; Leysen, R. A Review of Pressure-driven Membrane Processes in Wastewater Treatment and Drinking Water Production. *Environ. Prog.* **2003**, *22* (1), 46–56. <https://doi.org/10.1002/ep.670220116>.
- (12) Zhou, W.; Deng, J.; Qin, Z.; Huang, R.; Wang, Y.; Tong, S. Construction of MoS₂ Nanoarrays and MoO₃ Nanobelts: Two Efficient Adsorbents for Removal of Pb(II), Au(III) and Methylene Blue. *Journal of Environmental Sciences* **2022**, *111*, 38–50. <https://doi.org/10.1016/j.jes.2021.02.031>.
- (13) Yuan, C.; Weng, C.-H. Electrokinetic Enhancement Removal of Heavy Metals from Industrial Wastewater Sludge. *Chemosphere* **2006**, *65* (1), 88–96. <https://doi.org/10.1016/j.chemosphere.2006.02.050>.
- (14) Jasim, A. Q.; Ajjam, S. K. Removal of Heavy Metal Ions from Wastewater Using Ion Exchange Resin in a Batch Process with Kinetic Isotherm. *South African Journal of Chemical Engineering* **2024**, *49*, 43–54. <https://doi.org/10.1016/j.sajce.2024.04.002>.
- (15) Manos, M. J.; Kanatzidis, M. G. Highly Efficient and Rapid Cs⁺ Uptake by the Layered Metal Sulfide K_{2x}Mn_xSn_{3-x}S₆ (KMS-1). *J. Am. Chem. Soc.* **2009**, *131* (18), 6599–6607. <https://doi.org/10.1021/ja900977p>.
- (16) Mertz, J. L.; Fard, Z. H.; Malliakas, C. D.; Manos, M. J.; Kanatzidis, M. G. Selective Removal of Cs⁺, Sr²⁺, and Ni²⁺ by K_{2x}Mg_xSn_{3-x}S₆ ($x = 0.5-1$) (KMS-2) Relevant to Nuclear Waste Remediation. *Chem. Mater.* **2013**, *25* (10), 2116–2127. <https://doi.org/10.1021/cm400699r>.
- (17) Sarma, D.; Malliakas, C. D.; Subrahmanyam, K. S.; Islam, S. M.; Kanatzidis, M. G. K_{2x}Sn_{4-x}S_{8-x} ($x = 0.65-1$): A New Metal Sulfide for Rapid and Selective Removal of Cs⁺, Sr²⁺ and UO₂²⁺ Ions. *Chem. Sci.* **2016**, *7* (2), 1121–1132. <https://doi.org/10.1039/C5SC03040D>.
- (18) Alam, R.; Roy, S. C.; Islam, T.; Feng, R.; Zhu, X.; Donley, C. L.; Islam, S. M. Molybdenum-Oxysulfide-Functionalized MgAl-Layered Double Hydroxides—A Sorbent for Selenium Oxoanions. *Inorg. Chem.* **2024**, *63* (24), 10997–11005. <https://doi.org/10.1021/acs.inorgchem.4c00307>.
- (19) Ali Khan, M.; Wen, J. Evaluation of Physicochemical and Heavy Metals Characteristics in Surface Water under Anthropogenic Activities Using Multivariate Statistical Methods, Garra River, Ganges Basin, India. *Environmental Engineering Research* **2020**, *26* (6), 200280–0. <https://doi.org/10.4491/eer.2020.280>.
- (20) Blanchard, G.; Maunaye, M.; Martin, G. Removal of Heavy Metals from Waters by Means of Natural Zeolites. *Water Research* **1984**, *18* (12), 1501–1507. [https://doi.org/10.1016/0043-1354\(84\)90124-6](https://doi.org/10.1016/0043-1354(84)90124-6).
- (21) Jiménez-Castañeda, M.; Medina, D. Use of Surfactant-Modified Zeolites and Clays for the

- Removal of Heavy Metals from Water. *Water* **2017**, *9* (4), 235. <https://doi.org/10.3390/w9040235>.
- (22) Uchimiya, M.; Lima, I. M.; Thomas Klasson, K.; Chang, S.; Wartelle, L. H.; Rodgers, J. E. Immobilization of Heavy Metal Ions (Cu^{II} , Cd^{II} , Ni^{II} , and Pb^{II}) by Broiler Litter-Derived Biochars in Water and Soil. *J. Agric. Food Chem.* **2010**, *58* (9), 5538–5544. <https://doi.org/10.1021/jf9044217>.
- (23) Maneechakr, P.; Mongkollertlop, S. Investigation on Adsorption Behaviors of Heavy Metal Ions (Cd^{2+} , Cr^{3+} , Hg^{2+} and Pb^{2+}) through Low-Cost/Active Manganese Dioxide-Modified Magnetic Biochar Derived from Palm Kernel Cake Residue. *Journal of Environmental Chemical Engineering* **2020**, *8* (6), 104467. <https://doi.org/10.1016/j.jece.2020.104467>.
- (24) Lezzi, A.; Cobianco, S.; Roggero, A. Synthesis of Thiol Chelating Resins and Their Adsorption Properties toward Heavy Metal Ions. *J. Polym. Sci. A Polym. Chem.* **1994**, *32* (10), 1877–1883. <https://doi.org/10.1002/pola.1994.080321008>.
- (25) Mahmoud, M. E.; Kenawy, I. M. M.; Hafez, M. A. H.; Lashein, R. R. Removal, Preconcentration and Determination of Trace Heavy Metal Ions in Water Samples by AAS via Chemically Modified Silica Gel N-(1-Carboxy-6-Hydroxy) Benzylidenepropylamine Ion Exchanger. *Desalination* **2010**, *250* (1), 62–70. <https://doi.org/10.1016/j.desal.2009.09.009>.
- (26) Blanton, A.; Islam, T.; Roy, S. C.; Celik, A.; Nie, J.; Baker, D. R.; Li, D.; Taylor-Pashow, K.; Zhu, X.; Pramanik, A.; Amin, R.; Feng, R.; Chernikov, R.; Islam, S. M. Porous Semiconducting K–Sn–Mo–S Aerogel: Synthesis, Local Structure, and Ion-Exchange Properties. *Chem. Mater.* **2023**, *35* (24), 10446–10456. <https://doi.org/10.1021/acs.chemmater.3c01675>.
- (27) Pearson, R. G. **Hard and Soft Acids and Bases**. *J. Am. Chem. Soc.* **1963**, *85* (22), 3533–3539. <https://doi.org/10.1021/ja00905a001>.
- (28) Manos, M. J.; Kanatzidis, M. G. Sequestration of Heavy Metals from Water with Layered Metal Sulfides. *Chemistry A European J* **2009**, *15* (19), 4779–4784. <https://doi.org/10.1002/chem.200900353>.
- (29) Manos, M. J.; Petkov, V. G.; Kanatzidis, M. G. $\text{H}_{2x}\text{Mn}_x\text{Sn}_{3-x}\text{S}_6$ ($x = 0.11\text{--}0.25$): A Novel Reusable Sorbent for Highly Specific Mercury Capture Under Extreme pH Conditions. *Adv Funct Materials* **2009**, *19* (7), 1087–1092. <https://doi.org/10.1002/adfm.200801563>.
- (30) Manos, M. J.; Chrissafis, K.; Kanatzidis, M. G. Unique Pore Selectivity for Cs^+ and Exceptionally High NH_4^+ Exchange Capacity of the Chalcogenide Material $\text{K}_6\text{Sn}[\text{Zn}_4\text{Sn}_4\text{S}_{17}]$. *J. Am. Chem. Soc.* **2006**, *128* (27), 8875–8883. <https://doi.org/10.1021/ja061342t>.
- (31) Wang, K.-Y.; Feng, M.-L.; Huang, X.-Y.; Li, J. Organically Directed Heterometallic Chalcogenidometalates Containing Group 12(II)/13(III)/14(IV) Metal Ions and Antimony(III). *Coordination Chemistry Reviews* **2016**, *322*, 41–68. <https://doi.org/10.1016/j.ccr.2016.04.021>.
- (32) Oh, Y.; Bag, S.; Malliakas, C. D.; Kanatzidis, M. G. Selective Surfaces: High-Surface-Area Zinc Tin Sulfide Chalcogels. *Chem. Mater.* **2011**, *23* (9), 2447–2456. <https://doi.org/10.1021/cm2003462>.
- (33) Pala, I. R.; Brock, S. L. ZnS Nanoparticle Gels for Remediation of Pb^{2+} and Hg^{2+} Polluted

- Water. *ACS Appl. Mater. Interfaces* **2012**, *4* (4), 2160–2167. <https://doi.org/10.1021/am3001538>.
- (34) Gacoin, T.; Malier, L.; Counio, G.; Boilot, J.-P. CdS Nanoparticles and the Sol-Gel Process; Dunn, B. S., Mackenzie, J. D., Pope, E. J. A., Schmidt, H. K., Yamane, M., Eds.; San Diego, CA, 1997; pp 358–365. <https://doi.org/10.1117/12.284132>.
- (35) Mohanan, J. L.; Arachchige, I. U.; Brock, S. L. Porous Semiconductor Chalcogenide Aerogels. *Science* **2005**, *307* (5708), 397–400. <https://doi.org/10.1126/science.1106525>.
- (36) Bag, S.; Kanatzidis, M. G. Chalcogels: Porous Metal–Chalcogenide Networks from Main-Group Metal Ions. Effect of Surface Polarizability on Selectivity in Gas Separation. *J. Am. Chem. Soc.* **2010**, *132* (42), 14951–14959. <https://doi.org/10.1021/ja1059284>.
- (37) Manos, M. J.; Kanatzidis, M. G. Metal Sulfide Ion Exchangers: Superior Sorbents for the Capture of Toxic and Nuclear Waste-Related Metal Ions. *Chem. Sci.* **2016**, *7* (8), 4804–4824. <https://doi.org/10.1039/C6SC01039C>.
- (38) Nie, J.; Islam, T.; Roy, S. C.; Li, D.; Amin, R.; Taylor-Pashow, K.; Zhu, X.; Feng, R.; Chernikov, R.; Pramanik, A.; Han, F. X.; Kumbhar, A. S.; Islam, S. M. Amorphous K–Co–Mo–S_x Chalcogel: A Synergy of Surface Sorption and Ion-Exchange. *Small* **2024**, 2400679. <https://doi.org/10.1002/smll.202400679>.
- (39) Celik, A.; Baker, D. R.; Arslan, Z.; Zhu, X.; Blanton, A.; Nie, J.; Yang, S.; Ma, S.; Han, F. X.; Islam, S. M. Highly Efficient, Rapid, and Concurrent Removal of Toxic Heavy Metals by the Novel 2D Hybrid LDH–[Sn₂S₆]. *Chemical Engineering Journal* **2021**, *426*, 131696. <https://doi.org/10.1016/j.cej.2021.131696>.
- (40) Ma, L.; Wang, Q.; Islam, S. M.; Liu, Y.; Ma, S.; Kanatzidis, M. G. Highly Selective and Efficient Removal of Heavy Metals by Layered Double Hydroxide Intercalated with the MoS₄²⁻ Ion. *J. Am. Chem. Soc.* **2016**, *138* (8), 2858–2866. <https://doi.org/10.1021/jacs.6b00110>.
- (41) US EPA, O. *National Primary Drinking Water Regulations*. <https://www.epa.gov/ground-water-and-drinking-water/national-primary-drinking-water-regulations> (accessed 2023-11-20).
- (42) CPCB | Central Pollution Control Board. <https://cpcb.nic.in/who-guidelines-for-drinking-water-quality/> (accessed 2023-11-20).
- (43) Freundlich, H. Über Die Adsorption in Lösungen. *Zeitschrift für Physikalische Chemie* **1907**, *57U* (1), 385–470. <https://doi.org/10.1515/zpch-1907-5723>.
- (44) Langmuir, I. THE ADSORPTION OF GASES ON PLANE SURFACES OF GLASS, MICA AND PLATINUM. *J. Am. Chem. Soc.* **1918**, *40* (9), 1361–1403. <https://doi.org/10.1021/ja02242a004>.
- (45) Yang, L.; Xie, L.; Chu, M.; Wang, H.; Yuan, M.; Yu, Z.; Wang, C.; Yao, H.; Islam, S. M.; Shi, K.; Yan, D.; Ma, S.; Kanatzidis, M. G. Mo₃S₁₃²⁻ Intercalated Layered Double Hydroxide: Highly Selective Removal of Heavy Metals and Simultaneous Reduction of Ag⁺ Ions to Metallic Ag⁰ Ribbons. *Angew Chem Int Ed* **2022**, *61* (1), e202112511. <https://doi.org/10.1002/anie.202112511>.
- (46) Shao, P.; Chang, Z.; Li, M.; Lu, X.; Jiang, W.; Zhang, K.; Luo, X.; Yang, L. Mixed-Valence Molybdenum Oxide as a Recyclable Sorbent for Silver Removal and Recovery from

- Wastewater. *Nat Commun* **2023**, *14* (1), 1365. <https://doi.org/10.1038/s41467-023-37143-2>.
- (47) *MoS₄ 2- intercalated NiFeTi LDH as an efficient and selective adsorbent for elimination of heavy metals* - *RSC Advances* (RSC Publishing) DOI:10.1039/D0RA02766A. <https://pubs.rsc.org/en/content/articlehtml/2020/ra/d0ra02766a> (accessed 2020-11-01).
- (48) Ali, J.; Wang, H.; Ifthikar, J.; Khan, A.; Wang, T.; Zhan, K.; Shahzad, A.; Chen, Z.; Chen, Z. Efficient, Stable and Selective Adsorption of Heavy Metals by Thio-Functionalized Layered Double Hydroxide in Diverse Types of Water. *Chemical Engineering Journal* **2018**, *332*, 387–397. <https://doi.org/10.1016/j.cej.2017.09.080>.
- (49) Ma, L.; Wang, Q.; Islam, S. M.; Liu, Y.; Ma, S.; Kanatzidis, M. G. Highly Selective and Efficient Removal of Heavy Metals by Layered Double Hydroxide Intercalated with the MoS₄²⁻ Ion. *J. Am. Chem. Soc.* **2016**, *138* (8), 2858–2866. <https://doi.org/10.1021/jacs.6b00110>.
- (50) Xie, L.; Yu, Z.; Islam, S. M.; Shi, K.; Cheng, Y.; Yuan, M.; Zhao, J.; Sun, G.; Li, H.; Ma, S.; Kanatzidis, M. G. Remarkable Acid Stability of Polypyrrole-MoS₄: A Highly Selective and Efficient Scavenger of Heavy Metals Over a Wide pH Range. *Advanced Functional Materials* **2018**, *28* (20), 1800502. <https://doi.org/10.1002/adfm.201800502>.
- (51) Yuan, M.; Yao, H.; Xie, L.; Liu, X.; Wang, H.; Islam, S. M.; Shi, K.; Yu, Z.; Sun, G.; Li, H.; Ma, S.; Kanatzidis, M. G. Polypyrrole–MoS₄: An Efficient Sorbent for the Capture of Hg²⁺ and Highly Selective Extraction of Ag⁺ over Cu²⁺. *J. Am. Chem. Soc.* **2020**, *142* (3), 1574–1583. <https://doi.org/10.1021/jacs.9b12196>.
- (52) Jawad, A.; Liao, Z.; Zhou, Z.; Khan, A.; Wang, T.; Ifthikar, J.; Shahzad, A.; Chen, Z.; Chen, Z. Fe-MoS₄: An Effective and Stable LDH-Based Adsorbent for Selective Removal of Heavy Metals. *ACS Appl. Mater. Interfaces* **2017**, *9* (34), 28451–28463. <https://doi.org/10.1021/acsami.7b07208>.
- (53) *High and fast adsorption of Cd(II) and Pb(II) ions from aqueous solutions by a waste biomass based hydrogel* - ProQuest. <https://search.proquest.com/openview/5d999bad25cbeb28e244fc17e02ebdb3/1?pq-origsite=gscholar&cbl=2041939> (accessed 2020-11-01).
- (54) Ogawa, M.; Saito, F. Easily Oxidizable Polysulfide Anion Occluded in the Interlayer Space of Mg/Al Layered Double Hydroxide. *Chem. Lett.* **2004**, *33* (8), 1030–1031. <https://doi.org/10.1246/cl.2004.1030>.
- (55) *Efficient Removal of Heavy Metal Ions with An EDTA Functionalized Chitosan/Polyacrylamide Double Network Hydrogel* | *ACS Sustainable Chemistry & Engineering*. <https://pubs.acs.org/doi/abs/10.1021/acssuschemeng.6b02181> (accessed 2020-11-01).
- (56) Huang, G.; Wang, D.; Ma, S.; Chen, J.; Jiang, L.; Wang, P. A New, Low-Cost Adsorbent: Preparation, Characterization, and Adsorption Behavior of Pb(II) and Cu(II). *Journal of Colloid and Interface Science* **2015**, *445*, 294–302. <https://doi.org/10.1016/j.jcis.2014.12.099>.
- (57) *Versatile Cellulose-Based Carbon Aerogel for the Removal of Both Cationic and Anionic Metal Contaminants from Water* | *ACS Applied Materials & Interfaces*. <https://pubs.acs.org/doi/abs/10.1021/acsami.5b08287> (accessed 2020-11-01).

- (58) Hassanzadeh Fard, Z.; Malliakas, C. D.; Mertz, J. L.; Kanatzidis, M. G. Direct Extraction of Ag^+ and Hg^{2+} from Cyanide Complexes and Mode of Binding by the Layered $\text{K}_2\text{MgSn}_2\text{S}_6$ (KMS-2). *Chem. Mater.* **2015**, *27* (6), 1925–1928. <https://doi.org/10.1021/acs.chemmater.5b00374>.
- (59) Li, F.; Wang, X.; Yuan, T.; Sun, R. A Lignosulfonate-Modified Graphene Hydrogel with Ultrahigh Adsorption Capacity for $\text{Pb}(\text{II})$ Removal. *J. Mater. Chem. A* **2016**, *4* (30), 11888–11896. <https://doi.org/10.1039/C6TA03779H>.
- (60) Bao, J.; Fu, Y.; Bao, Z. Thiol-Functionalized Magnetite/Graphene Oxide Hybrid as a Reusable Adsorbent for Hg^{2+} Removal. *Nanoscale Research Letters* **2013**, *8* (1), 486. <https://doi.org/10.1186/1556-276X-8-486>.
- (61) Subrahmanyam, K. S.; Malliakas, C. D.; Sarma, D.; Armatas, G. S.; Wu, J.; Kanatzidis, M. G. Ion-Exchangeable Molybdenum Sulfide Porous Chalcogel: Gas Adsorption and Capture of Iodine and Mercury. *J. Am. Chem. Soc.* **2015**, *137* (43), 13943–13948. <https://doi.org/10.1021/jacs.5b09110>.
- (62) *X-ray Photoelectron Spectroscopy (XPS) Reference Pages Potassium*. <https://www.xpsfitting.com/2020/02/potassium.html>.
- (63) Moulder, J. F.; Stickle, W. F.; Sobol, P. E.; Bomben, K. D. *Handbook of X-Ray Photoelectron Spectroscopy*; Perkin-Elmer Corporation, 1992.
- (64) Roy, S. C.; Asaduzzaman, A.; May, B.; Beals, A. M.; Chen, X.; Zhu, X.; Islam, S. M. Oxidative Immobilization of Gaseous Mercury by $[\text{Mo}_3\text{S}(\text{S}_2)_6]^{2-}$ -Functionalized Layered Double Hydroxide. *Chem. Mater.* **2024**, *36* (11), 5826–5835. <https://doi.org/10.1021/acs.chemmater.4c01098>.
- (65) Trung, T. N.; Kim, D.-O.; Kim, E.-T. Direct and Self-Selective Synthesis of Ag Nanowires on Patterned Graphene. *RSC Adv.* **2017**, *7* (28), 17325–17331. <https://doi.org/10.1039/C6RA28389F>.

Data availability Statement

Data for this article, entitled “Ion Exchangeable K-Co-Mo-S_x Chalcogel — High Capacity Removal of Pb²⁺ and Ag⁺ and their Underlying Mechanisms” including material Characterization, heavy metal removal performance sorption kinetics, and capacity have been included as part of the Supplementary Information and others data are available at S. M. Islam, email: Muhammad.s.islam@jsums.edu.

Corresponding Author

Saiful M. Islam

Department of Chemistry, Physics, and Atmospheric Sciences

Jackson State University

Jackson, Mississippi-39217, USA